An Experimental Study on Air Leakage and Heat Transfer Characteristics of a Rotary-type Heat Recovery Ventilator

Hwataik Han†, Min-Kyu Kim*
School of Mechanical and Automotive Engineering, Kookmin University, Seoul 136-702, Korea
**Graduate School, Kookmin University, Seoul 136-702, Korea*

Key words: Air-to-air heat exchanger, Heat recovery, Rotary type, Carryover leakage, Pressure leakage

ABSTRACT: This study investigates the air leakage and heat transfer characteristics of a commercially available rotary-type air-to-air heat exchanger with a fiber polyester matrix. Crossover leakage between the exhaust and supply air is measured using a tracer gas method for various ventilation rates and rotational speeds of the wheel. A correlation equation for the leakage is obtained by summing up pressure leakage and carryover leakage. The pressure leakage is observed to be a function of ventilation rate only, and the carryover leakage is found to be a linear function of wheel speed. The real efficiency of the heat exchanger can be obtained from its apparent efficiency by taking into account the leakage ratio. The heat recovery efficiency decreases, as the ventilation rate increases. As the wheel speed increases, however, the efficiency increases initially but reaches a constant value for the speeds over 10 rpm.

Nomenclature

A_{gap}	: gap area for crossover [m^2]
C	: concentration of tracer gas [ppm]
E	: leakage ratio
f	: rotational speed of wheel [1/s]
q	: leakage airflow rate [m^3/s]
Q	: ventilation rate [m^3/s, CMH]
T	: temperature [℃]
V	: face velocity through matrix [m/s]
V_{matrix}	: matrix volume [m^3]

Greek symbols

η	: heat recovery efficiency
$\triangle P$	: pressure drop [Pa]
σ	: porosity of matrix

Subscripts

c	: carry-over leakage
EA	: exhaust air
eff	: effective
OA	: outdoor air
p	: pressure leakage
RA	: return air
SA	: supply air

† Corresponding author
Tel.: +82-2-910-4687; fax: +82-2-910-4839
E-mail address: hhan@kookmin.ac.kr

1. Introduction

Heat recovery ventilators are used to retrieve waste energy from exhaust air. An HRV is basically an air-to-air heat exchanger, the generic types of which include a fixed plate type, a rotary wheel type, a heat pipe type, and etc depending on heat transfer mechanism.[1]

A rotary wheel regenerator is often called an energy wheel or a heat wheel. It has been commonly utilized since versatile materials can be used as porous matrix or honeycomb. Crossover leakage may occur intrinsically, however, through the gaps around the rotating wheel. The cross contamination may be a significant problem in case exhaust gas is toxic or harmful. Moreover, the air leakage causes reduction in heat recovery efficiency.

There are extensive studies on the heat and moisture transfer performances of rotary wheels.[2,3] Tae et al.[4] have investigated the performance of porous polyurethane foam matrix experimentally, and Choi et al.[5] proposed a design method of optimization for rotary heat exchangers. However, there is a few studies on the leakage characteristics of the rotary wheels. Shah and Skiepko[6] categorized leakage paths and investigated the effects of leakage on heat transfer performance. Shang et al.[7] measured the air leakage rate and investigated its experimental uncertainties. Various shapes and materials are used for rotary wheels, and the leakage characteristics depend on operating conditions such as airflow rate and wheel speed. There are few studies on the effects of these parameters. It is the objective of the present study to investigate the leakage characteristics due to airflow rate and wheel speed, and the effects of the leakage on the real heat recovery efficiency of a rotary wheel ventilator.

2. Leakage around rotary wheel

There are various air paths crossing over a wheel as are shown in Fig. 1. As the wheel rotates, the air contained in void spaces is carried over to the other side of the wheel. It is called as the carryover leakage. The other leakage is the pressure leakage which takes place through the gaps by the pressure difference. Total air leakage is the sum of these leakages.

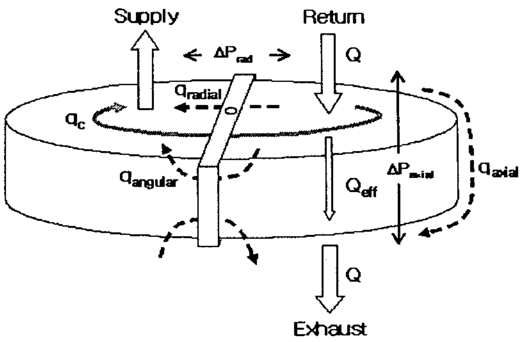

Fig. 1 Various air leakage paths around a rotating wheel.

$$q = q_c + q_p \tag{1}$$

The pressure leakage can be further categorized into radial leakage and angular leakage depending on its direction.

$$q_p = q_{radial} + q_{angular} \tag{2}$$

Axial leakage takes place along the flow direction through the side gaps around the wheel, which is also called peripheral leakage. However, it is not included in the crossover leakage. It merely reduces the effective airflow rate through the matrix and hence the heat recovery from the matrix. In case the supply and return airflow rates are in balance, the relation between leakage rates and effective airflow rate can be expressed as followings.

$$Q_{eff} + q_{axial} = Q - (q_c + q_p) \tag{3}$$

3. Experimental apparatus and procedure

A test apparatus has been prepared according to the ASHRAE Standard.[8] The ventilation unit has an exterior dimension of 570 mm × 590 mm × 420 mm. The radius and thickness of the rotary wheel are 230 mm and 40 mm, respectively. The wheel has six divisions for pieces of matrix. It is rotated by a rubber belt driven by a motor of 25 W in power consumption. The matrix is made of polyester fiber of 75 μm in diameter. The density of the fiber is 1,380 kg/m^3, and the porosity is 0.90 approximately.

Figure 2 shows the overall schematic of the experimental setup. Airflow rates in ducts are measured using nozzles of 60 mm in diameter (KS ISA 1932), connected to micro manometers (FCO332, precision ±0.5%).

Airflow rates are controlled by the inverters connected to fans. The *OA* duct is connected to an air-handling chamber which is maintained at the outdoor weather conditions. Temperatures are measured with T-type thermocouples, and their accuracies are within ±0.1 ℃. The experimental conditions are shown in Table 1.[9]

The SF_6 gas of 50% is used as a tracer gas to measure leakage ratios. The tracer gas is injected continuously into the *RA* duct and the concentrations are measured in the *SA* duct. The leakage ratio is calculated from the Eq. (4). The gas monitor works on the principle of infra-red absorption depending on the concentration. The detailed specifications can be found in the literature.[9]

$$E = \frac{C_{SA} - C_{OA}}{C_{RA} - C_{OA}} \tag{4}$$

The leakage rate is obtained from the leakage ratio multiplied by the supply airflow rate.

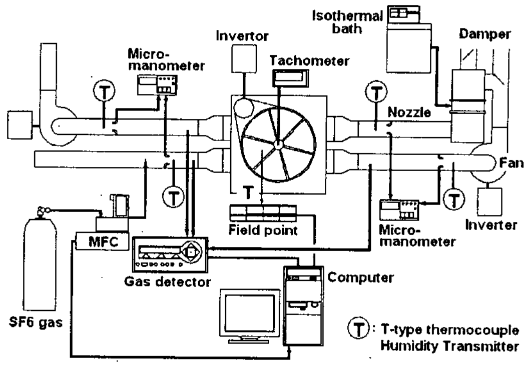

Fig. 2 Overall schematic diagram of the experimental setup.

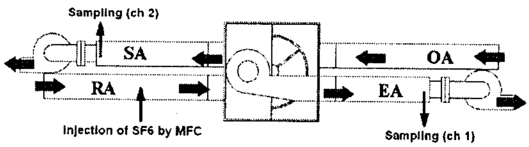

Fig. 3 Tracer gas experiment for leakage measurements.

$$q = Q_{SA} \cdot E \tag{5}$$

The apparent heat recovery efficiency is obtained from the temperatures measured at *SA*, *RA*, and *OA* ducts.

$$\eta_T = \frac{T_{SA} - T_{OA}}{T_{RA} - T_{OA}} \tag{6}$$

The real heat recovery efficiency can be calculated from Eq. (7), taken into account the leakage ratio, *E*.

$$\eta_{eff} = \frac{\eta_{apparent} - E}{1 - E} \tag{7}$$

Table 1 Experimental conditions

Parameters	Experimental conditions
Airflow rate	42~318 CMH (0.0117~0.0883 m^3/s)
Wheel speed	0~30 rpm (0~0.5 rps)
Indoor air temperature	27±0.3℃ : cooling, 21±0.3℃ : heating
Outdoor air temperature	35±0.3℃ : cooling, 7±0.3℃ : heating
Flow arrangement	Counterflow

4. Results and discussions

4.1 Matrix pressure characteristics

Figure 4 shows the pressure characteristics of the matrix of 150 mm in diameter and 40 mm in thickness. As the face velocity increases the pressure loss increases. The curve fitting by the Eq. (8) results in the exponent $m=1.60$.

$$\triangle P_{axial} = c V^{m} \tag{8}$$

The radial pressure drops ($\triangle P_{radial}$) and the axial pressure drops ($\triangle P_{axial}$) have been measured for various airflow rates of the ventilation unit. The ratio of the pressure drops are nearly constant ranging between 0.74 and 0.80, whose average is 0.776. The axial pressure drop characterizes the pressure loss through the matrix, and the radial pressure drop characterizes the cross air leakage.

4.2 Air leakage characteristics

The leakage ratio is shown in Fig. 5 according to the airflow rate and the wheel speed. The leakage ratio increases as the wheel speed increases, but decreases as the airflow rate increases. At 42 CMH, the maximum leakage ratio goes up to 50%.

The leakage rate is shown in Fig. 6, where

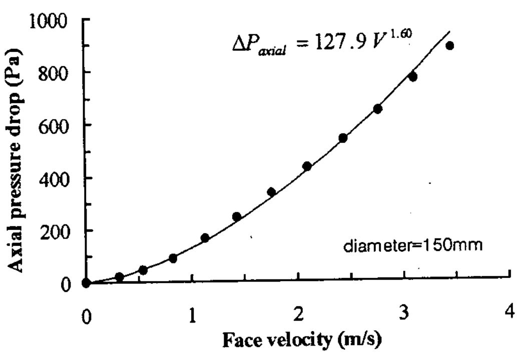

Fig. 4 Pressure drop across matrix with respect to face velocity.

the x-axis is in revolution per second, and the y-axis is in cubic meter per minute. It is interesting to observe the slopes are nearly constant regardless of the airflow rates, which is intrinsic to the carry-over leakage.

$$q_c = a \cdot f \tag{9}$$

where, the proportional constant, a, is $K_c \sigma \cdot V_{matrix}$, which is proportional to the matrix volume $V_{matrix}=0.006648\text{m}^3$ and the porosity $\sigma=0.90$.

The pressure leakage can be represented as a function of pressure difference in the radial direction.

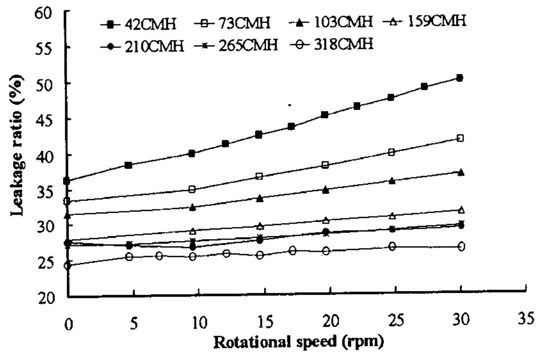

Fig. 5 Experimental results of leakage ratio.

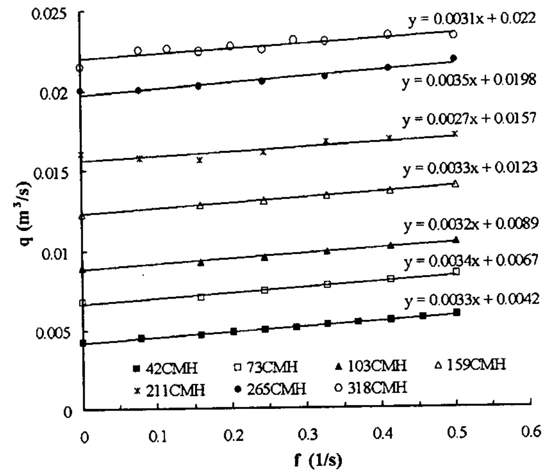

Fig. 6 Volumetric leakage airflow rate with respect to rotational speed of matrix.

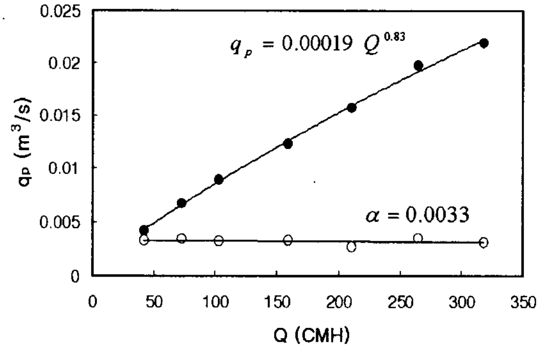

Fig. 7 Curve-fitting for pressure leakage q_p and proportional constant for carryover leakage.

$$q_P = K_P A_{gap} \Delta P_{radial}^{\frac{1}{n}} \qquad (10)$$

where A_{gap} is the gap area, ΔP_{radial} is the pressure difference in the radial direction, and K_p is a proportional constant. The pressure difference can be converted into that in the axial direction by using the pressure difference ratio defined previously. The leakage rate, finally, can be expressed as Eq. (11) in a functional form of the power exponent of the airflow rate using the pressure characteristics of the matrix.

$$q_p = \beta \cdot Q^{\frac{m}{n}} \qquad (11)$$

The leakage rate at zero speed indicates a pressure leakage. The slope indicates the proportional constant for carryover leakage. Curve-fitting results are shown in Fig. 7. Therefore, the total leakage rate q (CMS) can be expressed finally as a function of airflow rate Q (CMH) and rotational speed f (1/s) by combining Eq. (9) and Eq. (11).

$$q = 0.0033 f + 0.00019 Q^{0.83} \qquad (12)$$

4.3 Heat recovery efficiency

Figure 8 shows the heat recovery efficiency measured for heating and cooling conditions. As the wheel speed increases, the efficiency increases and becomes nearly constant over 10 rpm.

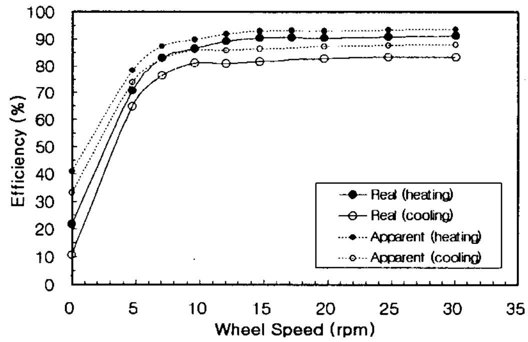

Fig. 8 Apparent and real efficiencies for heating and cooling conditions (318 CMH).

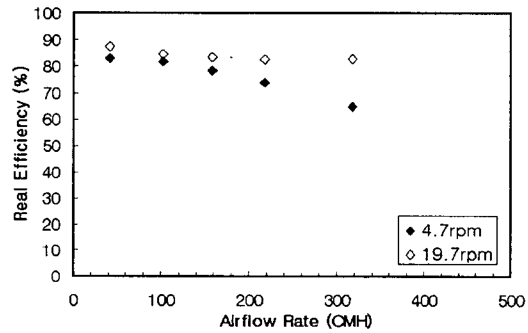

Fig. 9 Variations of real efficiency according to the airflow rate for cooling condition.

The cooling condition results in lower efficiency compared to the heating condition for all airflow rates. This is due to the heat generation by fan motors in the unit.

The dotted lines in the figure indicate real efficiencies compared to apparent efficiencies. They are 81~83% for cooling condition, and 87~81% for heating condition when the speed is over 10 rpm. The apparent and real efficiencies at zero speed are 40, 22% for heating condition, and 33, 11% for cooling condition, respectively. Notice the efficiency at zero speed is not zero, since there is heat transfer between two air streams by internal heat conduction.

The real heat recovery efficiency is shown in Fig. 9 according to the airflow rate. It is nearly constant with respect to the airflow rate for 20 rpm, whereas it is slightly decreasing for 5 rpm. For low flow rates, the efficiency is observed not to be affected by the wheel speed significantly.

5. Conclusions

This paper investigates the effects of airflow rate and wheel speed on the characteristics of air leakage and heat transfer of a rotary type heat recovery ventilator. Conclusions drawn from the experimental study are as follows.

(1) Total air leakage is the sum of pressure leakage which is a function of airflow rate only, and carryover leakage which is a function of wheel speed only.

(2) The pressure leakage increases with respect to the airflow rate, but it is constant with respect to the wheel speed. The carryover leakage is constant with respect to airflow rate, but it is proportional to the wheel speed.

(3) Heat recovery efficiency decreases as the airflow rate increases. It increases with respect to the rotational speed, but becomes nearly constant over a certain speed.

(4) The less the leakage rate is, the greater the effective efficiency is for a given apparent efficiency.

(5) Cooling conditions result in lower efficiency compared to heating conditions because of the internal heat generation from fan motors.

(6) Considering heat recovery efficiency, the optimal wheel speed is 10 rpm approximately for the present system.

The effect of cross air leakage is important in evaluating the performance of rotary type ventilators. In order to improve system performances, the system should be optimized with respect to the system parameters such as airflow rate and wheel speed. Further researches should be conducted on the effect of various parameters on the cross air leakage of rotary type ventilators.

Acknowledgement

This research has been supported by the research fund of Kookmin University in 2004.

References

1. ASHRAE, 1997, Handbook ASHRAE-Fundamentals, Atlanta, ASHRAE, Inc.
2. Simonson, C. J., Ciepliski, D. L. and Besant, R. W, 1999, Determining the performance of energy wheels: Part I-Experimental and numerical methods, ASHRAE Trans., Vol. 105, No. 1, pp. 177-187.
3. Simonson, C. J., Ciepliski, D. L. and Besant, R. W., 1999, Determining the performance of energy wheels: Part II-Experimental data and numerical validation, ASHRAE Trans., Vol. 105, No. 1, pp. 188-205.
4. Tae, C. S., Park, S. D., Cho, S. H. and Choi, Y. D., 1993, Experimental study on the performance of axial flow rotary heat exchanger with the porous polyurethane foam matrix, Korean Journal of Air-Conditioning and Refrigeration Engineering, Vol. 5, No. 1, pp. 45-54.
5. Choi, Y. D., Park, S. D., Woo, J. S. and Tae, C. S., 1991, A study on the optimum design of axial rotary sensible heat exchanger for the heat recovery of exhaust gas, Korean Journal of Air-Conditioning and Refrigeration Engineering, Vol. 3, No. 2, pp. 131-141.
6. Shah, R. K. and Skiepko, T., 1999, Influence of leakage distribution on the thermal performance of a rotary regenerator, Applied Thermal Engineering, pp. 685-705.
7. Shang, W., Wawryk, M. and Besant, R. W., Air crossover in rotary wheels used for air-to-air heat and moisture recovery, ASHRAE Trans., Vol. 107, pp. 72-83.
8. ASHRAE Standard, 1984, Method of Testing Air-to-Air Heat Exchanger, pp. 84-78.
9. Kim, M. K., 2003, An experimental study on the heat transfer characteristics of rotary-type total heat exchanger, MS thesis, Kookmin University, Seoul, Korea.